PAPER

NJC

www.rsc.org/njc

Unexpected chromogenic properties of 1,3,3-trimethylspiro(indoline-2,3′-[3*H*]naphtho [2,1-b][1,4]oxazine) in the solid phase: photochromism, piezochromism and acidichromism

Pier Luigi Gentili,[a] Morena Nocchetti,[b] Costanza Miliani[c] and Gianna Favaro*[a]

[a] *Laboratorio di Fotofisica e Fotochimica, Dipartimento di Chimica, Università di Perugia, 06123, Perugia, Italy. E-mail: favaro@unipg.it*

[b] *Laboratorio di Chimica Inorganica, Dipartimento di Chimica, Università di Perugia, 06123, Perugia, Italy*

[c] *CNR Istituto di Scienze e Tecnologie Molecolari, 06123, Perugia, Italy*

Received* (*in Montpellier, France*) *24th October 2003, Accepted 11th November 2003
First published as an Advance Article on the web 10th February 2004

New chromogenic properties of a spirooxazine {1,3,3-trimethylspiro(indoline-2,3′-[3*H*]naphtho[2,1-b][1,4]-oxazine), SO} are presented in this work. This molecule was found to be photochromic and piezochromic in the pure microcrystalline solid phase and also exhibited acidichromism when kept in contact with a hydrogen-donating solid phase. Photochromism was observed under continuous UV irradiation. Biexponential thermal bleaching followed the interruption of irradiation. Piezochromism was detected by applying a mechanical force to the solid powder, using either a hydraulic press or manual crushing. After discontinuing pressure, biexponential bleaching kinetics were observed. The biexponential nature of the fading processes is interpreted in terms of merocyanine (M) micro-spot formation inside the crystalline phase. The third chromogenic property of the solid spirooxazine, acidichromism, is due to the extraction of protons from an acidic solid matrix, alpha zirconium phosphate [α-$Zr(HPO_4)_2 \cdot H_2O$]. Proton transfer to SO in the solid phase causes the appearance of a purple colour. The spectral evolution is qualitatively similar to that observed in CH_3CN solution when $HClO_4$ is added at room temperature and in the dark. Temporal evolution of the colour bands, in both solid and liquid phases, is interpreted in terms of an initial protonation, inducing ring-opening, and a second protonation, leading to a colourless product.

Introduction

Chromogenic systems often exhibit surprising new behaviours that can find potential applications in optically switchable materials.[1] These molecular systems are sensitive to external perturbations of both a ''physical'' (heat, light, pressure or electric field) and ''chemical'' (complexing agents or pH variations) nature. These perturbations induce structural molecular transformations, whereby colour appears. The structural changes are often reversible; by interrupting the perturbation or applying a different one, the initial state and colour can be restored.

Chromogenism is classified according to the nature of the external perturbation: ''thermochromism'', if it is favoured by heating, ''photochromism'', if it is promoted by light, ''piezochromism'', if caused by a mechanical force, ''electrochromism'', if stimulated by an electric field and ''acidichromism'', if pH variations are responsible for colouration-decolouration processes. The neologisms ''coordination-chromism'' and metallochromism can be coined for colour changes produced by a complexation reaction.[2,3]

These materials have been receiving increasing attention because they can be used to improve display and optical storage technologies[4–7] and can be employed as signal transducers between the microscopic and macroscopic worlds. Overall, there are literally thousands of switchable chemical compounds in the three states of matter[1] but it is quite rare to observe more than one kind of chromogenism in the same material.

In this paper, unexpected chromogenic properties of 1,3,3-trimethylspiro(indoline-2,3′-[3*H*]naphtho[2,1-b][1,4]oxazine) (SO) in a microcrystalline pure solid phase are reported. They are compared and related to the chromogenic properties detectable in liquid solution.

It is well-known that SO exhibits photochromic,[8–11] thermochromic[11,12] and acidichromic[13,14] properties in solution and in various matrices. The photoproduced merocyanine (M) thermally reconverts to the original spiro isomer (Scheme 1). In an acidic solution,[13,14] the thermally induced ground state M becomes protonated (MH^+) and it absorbs in the visible region at higher energy with respect to M, due to reduced electronic delocalization.

In this work, SO was found to be (1) photochromic in a microcrystalline pure solid phase under steady UV irradiation, (2) piezochromic, under the action of a mechanical force applied by both hydraulic press and manual crushing and (3) acidichromic by contact with a powdery solid matrix, zirconium phosphate with alpha structure, having acidic hydroxyl groups on its surface that can release protons to basic centres of SO and M.

Photochromism and piezochromism in a pure crystalline phase are very unusual, due to the lack of free volume in the

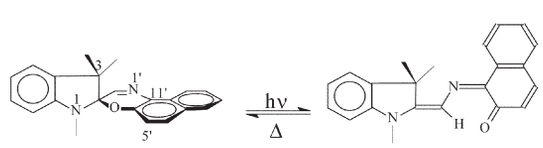

SO M

Scheme 1

DOI: 10.1039/b313637j

crystal lattice. In fact, even if photochromism and piezochromism were expected for two cationic spiropyrans in crystalline form,[15] spirooxazine and spiropyran powders have never been found to show colouration under either UV irradiation or pressure. Only recently, by using intense UV pulsed excitation (femtosecond time scale),[16,17] was photocolouration observed in solid SO and other spiro compounds. Under weak-intensity laser excitation, a non-planar open form was produced, which absorbed at low energy (around 740 nm) and thermally faded to the ground state spiro isomer without yielding the trans-planar M. In order to obtain the transoid planar structure, which absorbs around 600 nm, more intense irradiating light was needed.

With regard to acidichromism, this is the first time that solid SO, mixed with an acidic powder, was found to extract protons from the latter, with an enhanced efficiency upon crushing the mixture. The protonation of M causes a purple colour to appear whose saturation requires a relatively long time. To interpret this behaviour, SO acetonitrile solutions, acidified by adding various amounts of $HClO_4$, were investigated. Even though there have been several studies on SO acidichromism in solution,[13,14,18–20] a detailed kinetic study has never been reported. In this paper, the time-dependence of the acid-induced colouration in a solution is investigated and compared to the behaviour in the solid phase.

Experimental

Materials

1,3,3-Trimethylspiro(indoline-2,3′-[3*H*]naphtho[2,1-b][1,4]oxazine) was supplied by Great Lakes Chemical Italia s.r.l. for previous studies[11] and was used without further purification. The solvent, acetonitrile, CH_3CN, was a Fluka product.

Zirconium phosphate, $Zr(HPO_4)_2{\cdot}H_2O$ (ZrP), was synthesized according to the method in ref. 21. $ZrOCl_2{\cdot}8H_2O$ was dissolved in water; HF and H_3PO_4 were then added with stirring. After evaporation, a crystalline precipitate of $Zr(HPO_4)_2{\cdot}H_2O$ was obtained.[21]

Apparatus

The absorption spectra of the powdery samples, sandwiched between two quartz slides, were recorded using a Perkin–Elmer Lambda 16 spectrophotometer, equipped with a Perkin–Elmer accessory for reflectance measurements, or a home-made portable instrument equipped with a deuterium–halogen DH-2000-FHS lamp and an integrating sphere. A Hewlett–Packard 8453 diode array spectrophotometer was also used for the measurements in solution.

Corrected emission spectra were recorded using a Spex Fluorolog-2 1680/1 spectrofluorimeter, controlled by the Spex DM 3000F spectroscopy software. For measurements in polarized light, the Spex fluorimeter was equipped with an L-format polarization assembly with Glen–Thompson polarizers, model 1935B. The polarizers were matched to give 100% extinction.

For X-ray diffraction measurements, a computer-controlled Philips PW 1710 diffractometer with graphite-monochromated Cu–Kα radiation was used, operating at 40 kV, 30 mA, step-scan 0.03° 2θ and 1 s counting time.

Measurement conditions

To investigate photochromism, the irradiation was carried out with a high-pressure mercury lamp, filtered by a large-band filter, transmitting the 230–400 nm wavelength range. The powdery sample was packed into a spectrophotometric cell (0.1 cm path length). The kinetics of the thermal ring-closure reaction were spectrophotometrically recorded at a fixed wavelength, following the colour bleaching of the irradiated sample immediately after removing the irradiating source.

ZrP and SO powders were mixed in a 10:1 mass ratio and crushed in an agate mortar. X-Ray powder diffraction patterns of the microcrystalline solids were taken before and after crushing. Mechanical "static" force was applied on the powder by means of a hydraulic press (endowed with an oil pump); pressures around 240 atm were applied on different samples. After applying the pressure, the powder (in a 0.1 cm path length cell or sandwiched between two quartz slides) was spectrophotometrically analyzed and the thermal ring-closure kinetics were monitored.

To measure the emission from solid samples (0.1 cm path length), excitation and emission light was filtered through interferential and cut-on filters, respectively. The light emitted by the samples was collected at 22.5°. The polarized spectra were recorded adjusting the excitation polarizer parallel or perpendicular to the polarization plane of the emission polarizer. The polarized spectra and anisotropy traces were obtained using the four possible combinations of the excitation and emission polarization planes.

Known quantities of 0.116 M and 0.00116 M $HClO_4$ aqueous solutions (de-ionized and distilled water) were added to CH_3CN solutions of SO, $(6–5)\times10^{-5}$ M, in a spectrophotometric cell (3 ml). After the addition the solutions were shaken and the spectral evolution was recorded using a diode array spectrophotometer. To test the acidichromic reversibility, known quantities of 0.1 M and 0.001 M NaOH aqueous solutions were added to acid-equilibrated SO solutions.

The emission from solution was collected at a right angle. To measure fluorescence quantum yields, Φ_F, the corrected areas of the standard (anthracene in ethanol, $A = 0.005$ at 366 nm, previously calibrated with an absolute method[22]) and sample ($A \approx 0.005$, at 366 nm for SO and at 330 nm for the reaction product) emissions were compared and corrected for the refraction index of the medium. Different irradiation wavelengths were selected, using the fluorimeter excitation system with a band pass of 1.9–3.8 nm.

All measurements were carried out at room temperature (20 ± 2 °C).

Results and discussion

Spectral properties in the solid phase

1,3,3-Trimethylspiro(indoline-2,3′-[3*H*]naphtho[2,1-b][1,4]oxazine), SO, is a micro-crystalline powder whose particles have an average size of some ten μm, as estimated by scanning electron microscopy.

The absorption spectrum of the SO powder is shown in Fig. 1 in terms of the Kubelka–Munk function;[23] K is the

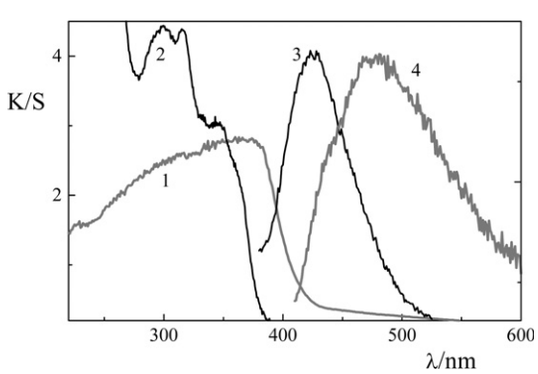

Fig. 1 Spectral properties of SO in a pure solid phase and in CH_3CN solution: (1) absorption spectrum of the solid SO in terms of the Kubelka–Munk function[23] (K/S); (2) absorption spectrum of SO in CH_3CN solution; (3) fluorescence spectrum of SO in CH_3CN; (4) fluorescence spectrum of SO in the solid phase.

absorption coefficient and S is the scattering coefficient. This spectrum shows a long tail in the visible region, up to 420 nm, that is responsible for the yellow colour of the solid. The powder exhibits a fluorescence band, centred at 479 nm (spectrum 4 of Fig. 1). SO shows fluorescence even in acetonitrile solution ($\lambda_{max} = 424$ nm, emission quantum yield 2.1×10^{-4} at $\lambda_{ex} = 315$ nm).

The broadening of the emission band observed in the solid ($\Delta\lambda_{1/2} = 140$ nm), compared to that in CH_3CN ($\Delta\lambda_{1/2} = 80$ nm), together with the larger Stokes shift in the solid than in the liquid, 5100 cm^{-1} and 4400 cm^{-1}, respectively, suggest that significant energy diffusion processes occur in the crystalline phase. These processes can be assigned to exciton-phonon interactions: the electronic excitation energy, localized in specific molecules, is partially degraded into lattice vibrations (heat) during energy migration through microcrystal sites. This model of incoherent migration of electronic excitation energy is experimentally confirmed by the low fluorescence anisotropy ($r < 0.10$) exhibited by SO powder.

Photochromism and piezochromism in the solid phase

Pure solid SO was found to be sensitive to both continuous UV irradiation and external pressure. In order to demonstrate the spectral changes induced by different external perturbations, the percentage absorption increment, $100[1 - (R/R_0)]$, is plotted as a function of wavelength in Fig. 2 (R_0 and R are the reflectance values before and immediately after perturbation, respectively).

Spectrum (1) of Fig. 2 was produced during prolonged UV irradiation (60 min) of solid SO with a high pressure Hg lamp. It shows a broad band with a maximum at 615 nm; the powder became blue. Spectrum (2) of Fig. 2 was obtained after about 225 atm of pressure were applied by hydraulic press for 12 min: a band with a maximum at 605 nm was generated and the percentage absorption increment was about half of that obtained by UV irradiation. Spectrum (3) of Fig. 2 resulted after the powder was manually crushed for 6 min in an agate mortar. This kind of perturbation, which is combined with a local heating effect due to friction, could be called "dynamic" piezochromism to distinguish it from that produced using a hydraulic press, which, in contrast, can be defined as "static" piezochromism. The absorption maximum is at 607 nm and the percentage absorption increment is about one-fourth of that produced by UV irradiation.

The positions of the colour bands obtained by irradiation and by pressure suggest that open planar merocyanines (Ms) are formed, which are characterized by an absorption around 600 nm, whereas open non-planar zwitterionic molecules absorb around 740 nm.[16] Since the bands observed in solid phase overlap, even if produced by different stimulations, they can be assigned to the same M isomer, surrounded by a similar micro-environment. The spectral properties of M in different media are summarized in Table 1. The position of the colour band detected in solid phase corresponds to that in a polar micro-environment; it is red-shifted compared with that in non-polar solvents. That is, the Ms in the microcrystalline phase are in a polar environment.

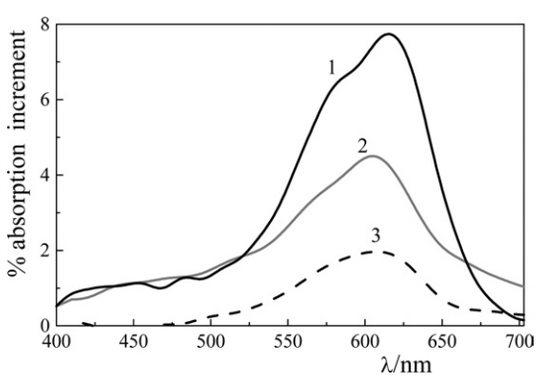

Fig. 2 Percentage absorption increments for SO powder after different perturbations: (1) UV irradiation; (2) pressure applied by a hydraulic press; (3) pressure produced by manual crushing.

The colour change induced by external perturbations is not permanent; when the perturbing action was discontinued, the band in the visible region thermally disappeared. The fading process is well-described by a biexponential function, as shown by the example reported in Fig. 3. For the purpose of comparison, in the insert of Fig. 3, the same kinetics is treated as a logarithm function: clearly, two components contribute to the thermal fading. The bleaching rate constants of the M produced in powdery samples by different perturbations are reported in Table 1, together with some data obtained in other media. The constants, k_1 and k_2, measured after the three different perturbations, are of the same order of magnitude; slight differences in their values depend on how the colour band was generated. The k_2 value (slow component) is four-to-five times smaller than k_1.

Based on these findings, a mechanistic interpretation of the SO powder chromogenism can be proposed. When C–O spiro bond breaking is induced by irradiation (photochromism), the tight arrangement of molecules in the solid phase does not allow free intramolecular rotation and hence a rapid ring-closure reaction converts the electromagnetic radiation energy into heat. Increased temperature induces wider molecular oscillations in the microcrystals. Thus, some excited SO molecules, after C–O cleavage, evolve towards the planar photomerocyanine structure, creating local disorder in the lattice that favours further formation of planar merocyanines in the neighbouring positions. Coloured micro-spots are progressively formed. If the perturbation is discontinued, they tend to disaggregate as a consequence of fading. The biexponential bleaching kinetics is probably due to different closure rates of M inside the spots (k_1) and at the spot borders (k_2). Since the spot interior loses crystalline character and has glassy-like structure, the internal Ms should be less constrained than the Ms at the spot borders, where an appreciable degree of crystallinity is maintained. This situation is schematically represented in Fig. 4. The hypothesis of the formation of M spots is in agreement with the red-shifted position of the colour band associated with the planar M. The bathochromic shift suggests that each M is located in a micro-environment having polar character, in which the high polarity is generated by the M molecules themselves. In fact, the dipole moment of M is about three times that of the closed structure.[27]

The piezochromism of the SO powder can be understood by considering that the interaction of the electron pair of the indoline nitrogen with the antibonding orbital of the C–O spiro bond is the driving force for the opening reaction.[28] This interaction can be enhanced by applying pressure, which forces the indoline and the naphthooxazine rings to be coplanar. Pressure also favours the SO → M conversion because it is

Table 1 Spectral (λ_{max}) and kinetic (k_1 and k_2) properties of M in various media at 293 K

Medium	λ_{max}/nm	k_1/s^{-1}	k_2/s^{-1}
Pure solid (photochromism)	615	0.0054	0.0010
Pure solid (static piezochromism)	605	0.0019	0.0004
Pure solid (dynamic piezochromism)	607	0.0033	0.0009
Ethanol[11]	613	0.041	—
Methylcyclohexane[11]	585	0.052	—
ZrC8 (zirconium phosphonate)[24]	610	0.014	0.0015
AOT (microemulsion)[25]	600	0.16	—
Gel[26]	613	0.15	—

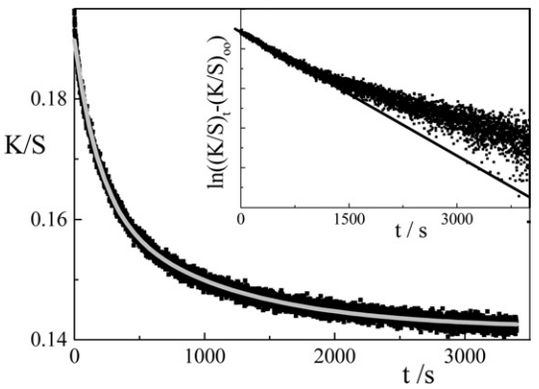

Fig. 3 Kinetics of the thermal fading process, followed at 610 nm, fitted by a biexponential function. Insert: logarithmic plot for the same kinetics.

accompanied by volume contraction. The biexponential nature of the fading process and the spectral position of the colour band suggest that spots of "piezo-merocyanines" could even be formed by applying a mechanical force. Reticular defects could act as "nucleation centres" for M spot formation, according to the principle that in a solid, subjected to an external stress, the force is concentrated into the defects. This suggests a new way to produce chromogenic solids with high colourability, by introducing many defects into the crystalline lattice. When SO powder is pressed by manual crushing, the friction produces a local temperature increase that is probably responsible for the k_1 and k_2 values being greater after the "dynamic" mechanical perturbation (*i.e.* after grinding) than after the "static" mechanical perturbation (hydraulic press). Interestingly, independently of how chromogenism was stimulated, the contribution of the fast component to the absorbance is only slightly larger (approximately by a factor of 1.3) than that of the slower component. Based on the proposed model, this means that the number of Ms inside the spots does not substantially exceed that at the spot borders.

By comparing the thermal bleaching constants in the pure microcrystalline solid phase with those obtained in other micro-environments (Table 1), it can be observed that the slowest fading processes were recorded in the pure solid phase. Due to significant structural transformations associated with the M → SO conversion, the ring-closure reaction is influenced by both the medium viscosity and the available free volume, and is also sensitive to medium polarity. A highly polar environment stabilizes the transition state of the closure reaction, thus increasing the rate constant for the thermal bleaching. As can be seen in Table 1, the polar effect overcomes the steric and viscosity effects in a gel,[26] and therefore the bleaching is faster. When M is adsorbed on a solid phase, $Zr[O_3PCH_2NHCH_2PO_3(CH_2)_7CH_3]F{\cdot}0{,}2H_2O$ (ZrC8),[24] rigidity effects overcome polar effects and the bleaching is slower. In the pure microcrystalline solid, the rigid three-dimensional molecular arrangement is the factor that greatly slows down the fading process. Furthermore, the ordered distribution of the reticular units creates an electrostatic force field that hinders molecular movements and hence M → SO conversion. This is also the reason why very intense perturbations (prolonged UV irradiation and strong pressure) are necessary to induce colouration in the pure solid.

Acidichromism in the solid phase

Serendipitously, it was found that the SO microcrystalline powder, in physical contact with an acidic solid matrix such as alpha zirconium phosphate, α-$Zr(HPO_4)_2{\cdot}H_2O$ (ZrP), can tear protons away.

ZrP has a layered structure[29] in which the metallic atoms lie nearly in a plane and are bridged by phosphate groups. Three of the oxygen atoms of phosphate are bonded to three different zirconium atoms arranged at the apices of a nearly equilateral triangle. The fourth oxygen atom points away from the layer and bonds to a hydrogen atom. The distance between adjacent layers is 7.56 Å. The mole number of POH acidic groups on each face of a lamella is 6.6×10^{-3} for 1 g and the free area associated with each group is 24 Å^2. ZrP is a well-known proton conductor.[30] Proton diffusion is not possible in the absence of adsorbed water molecules because the distance between neighbouring phosphate groups that belong to the same face of the layer is too large (5.30 Å).

Spectrum 1 of Fig. 5 was obtained from a powdery SO–ZrP mixture (mass ratio, 1:10). After 17 h, a broad band in the visible region grew (Fig. 5, spectrum 2). If the mixture was crushed for several minutes in an agate mortar, a purple colour appeared. It increased up to saturation, which was very visible. Spectrum 3 (Fig. 5), showing a broad band in the visible region centred at 540 nm, was recorded soon after the grinding; its intensity increased with time (spectrum 4, recorded 4 h after crushing). X-Ray diffraction analysis of the powdery sample, before and after crushing, showed that SO intercalation into the interlamellar regions of ZrP did not occur, at least within the sensitivity limits of this method. The interlayer distance remained at 7.56 Å. In the absence of any further perturbation, the absorption band very slowly decreased (spectrum 5, recorded 9 months after grinding).

By comparing the results with those obtained in solution,[13,14,18] the band in the visible region is assigned to the protonated planar merocyanine (MH^+). Protonation reduces the delocalization of the π-electron system, thus inducing a hypsochromic spectral shift compared to M. A small amount of MH^+ was formed after several hours of physical contact between ZrP and SO (Fig. 5, spectrum 2). Proton transfer

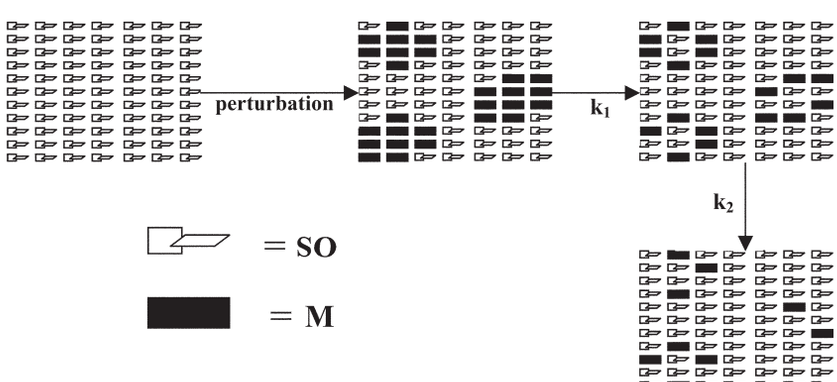

Fig. 4 Schematic illustration of the formation of M spots after external perturbation and the subsequent fading processes, characterized by different kinetic behaviours (k_1 and k_2).

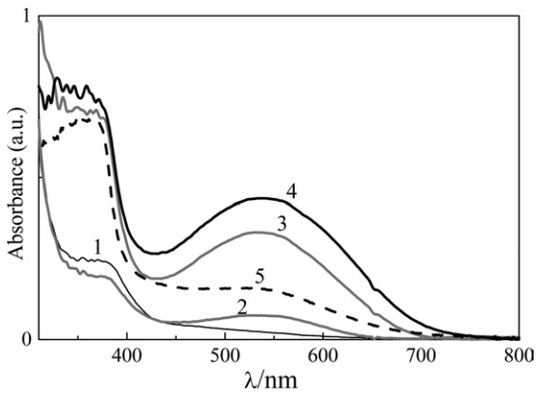

Fig. 5 Spectral modifications due to proton transfer from ZrP to SO in the solid phase: (1) spectrum of the two-powder system soon after mixing; (2) spectrum of the powdery mixture 17 h after mixing; (3) spectrum of the powdery mixture soon after crushing; (4) spectrum of the powdery mixture 4 h after crushing; (5) spectrum of the powdery mixture 9 months after crushing.

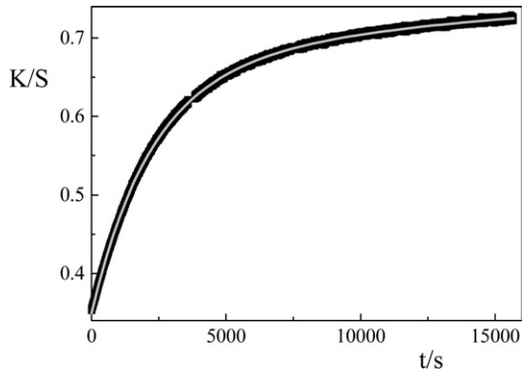

Fig. 6 Colour-enhancing kinetics of the powdery ZrP + SO mixture soon after crushing, fitted by a biexponential function (gray line).

occurs from the POH groups of the ZrP surface to the basic centres of SO, exploiting the hydration water of ZrP as a vehicle. Protonation of SO can induce a ring-opening reaction and formation of the planar MH^+ (Scheme 2).

If the powdery mixture was crushed, spots of planar Ms formed in the SO solid phase: the Ms slowly close, especially those at the spot borders. They can also easily undergo protonation, because they are stronger bases than SO. The colour-enhancing kinetics, recorded soon after crushing, fit a biexponential function well (Fig. 6). The fast component, $k_1 = (4.64 \pm 0.01) \times 10^{-4}$ s^{-1} is assigned to the proton transfer between the two solid phases; the Ms, produced by mechanical perturbation, is protonated. The slower component, $k_2 = (8.2 \pm 0.1) \times 10^{-5}$ s^{-1}, refers to the formation of MH^+ from SOH^+, which is the rate-determining step for the appearance of colour for the ZrP–SO mixture in the absence of any external mechanical perturbation.

After several hours, saturation is attained and proton transfer ceases. An extremely slow (several weeks) bleaching process starts by which MH^+ converts into the closed form and the colour band disappears (spectrum 5 of Fig. 5). The lower basicity of the closed form facilitates proton release to the anionic surface of ZrP.

Acidichromism in solution

The addition of a strong acid ($HClO_4$) to a solution of SO in CH_3CN, induced the appearance of a colour band, similar to that observed for acidichromism in the solid phase, but occurring over a different time scale since the solution turned purple instantaneously. The intensity of the colour band, centred at 511 nm (Fig. 7), first increased to a maximum and then slowly decayed. Therefore, the temporal evolution of the absorbance, followed at the maximum of the colour band, was constituted by two branches, one corresponding to colour forming and the other to colour bleaching (Fig. 8). The colour forming kinetics were independent of the acid concentration, while the decreasing trend, corresponding to colour fading, depended on the concentration of the added acid. Acidified SO solutions were spectrally and kinetically analyzed under two limiting conditions with the $HClO_4$:SO molar ratio equal to 0.5 or 50. In the former case, the decay kinetics were much slower than with excess acid (Fig. 8). Upon NaOH addition, the diluted acid solution reversibly became colourless, while the concentrated one irreversibly evolved, yielding a blue-shifted and more structured spectrum than that of the starting SO. The colour band has been assigned to the planar protonated merocyanine.[13,18]

In order to interpret the spectral evolution, the following reactions were taken into account:

– thermochromic equilibrium,

$$\mathrm{SO} \underset{k_{-1}}{\overset{k_1}{\rightleftharpoons}} \mathrm{M} \qquad (1)$$

– protonation of M, which is a stronger base than SO,

$$\mathrm{M} \xrightarrow{k_2(+\mathrm{H}^+)} \mathrm{MH}^+ \qquad (2)$$

– closure of the protonated MH^+ to SOH^+:

$$\mathrm{MH}^+ \xrightarrow{k_3} \mathrm{SOH}^+ \qquad (3)$$

– protonation to yield MH_2^{2+}:

$$\mathrm{MH}^+ + \mathrm{H}^+ \xrightarrow{k_4} \mathrm{MH}_2^{2+} \qquad (4)$$

– closure of MH_2^{2+} to form SOH_2^{2+}:

$$\mathrm{MH}_2^{2+} \xrightarrow{k_5} \mathrm{SOH}_2^{2+} \qquad (5)$$

When $HClO_4$ is added, to re-establish the thermochromic equilibrium in eqn. (1), SO continuously supplies M, which

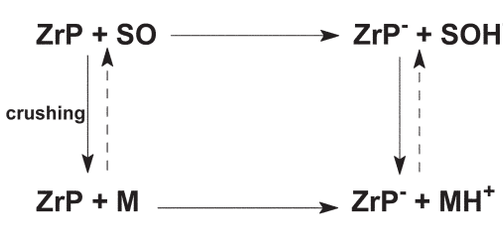

Scheme 2

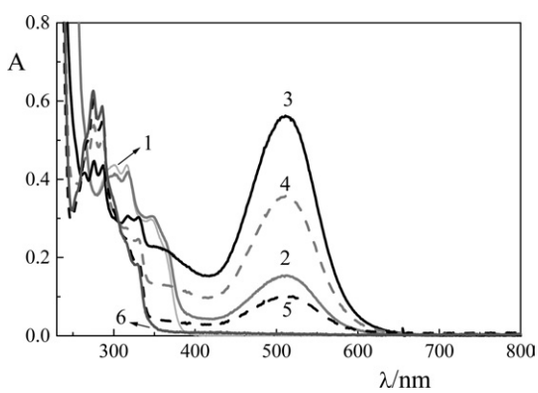

Fig. 7 Spectral evolution of SO in CH_3CN ($c \cong 10^{-5}$ M) induced by adding $(HClO_4)_{aq}$ in great excess (50:1 $HClO_4$:SO molar ratio): (1) before acid addition; (2) soon after addition; (3) 53 min after addition; (4) after 2 h and 11 min; (5) after 6 h and 28 min; (6) after 2 days.

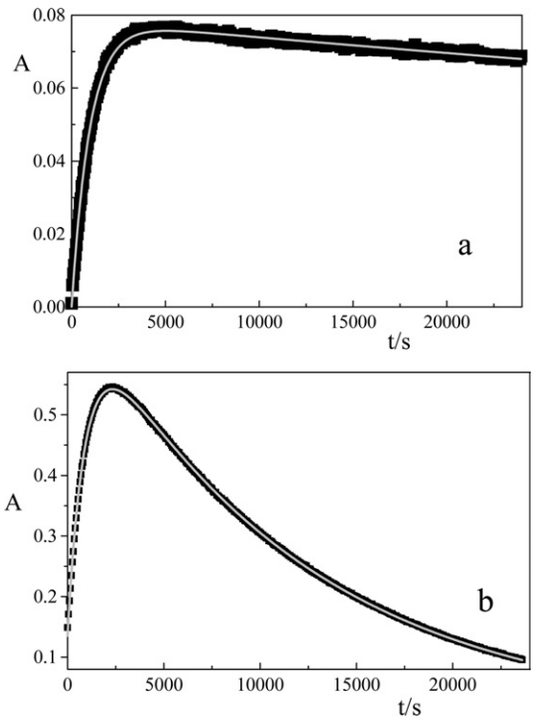

Fig. 8 Temporal evolution of the absorbance at 510 nm (MH^+ absorption), induced by adding $(HClO_4)_{aq}$ to an SO acetonitrile solution: (a) 1:2 $HClO_4$:SO molar ratio; (b) 50:1 $HClO_4$:SO molar ratio. The gray lines are fits to the kinetic expressions (see text).

is consumed in the protonation process in eqn. (2). If the amount of acid is insufficient, MH^+ slowly closes as in eqn. (3) while it undergoes protonation in eqn. (4) and subsequent closure to SOH_2^{2+} [eqn. (5)] when the acid is in excess. Since the M concentration remains small and constant, a steady-state approximation can be applied [eqn. (6)]. Considering the above processes [eqns. (1)–(5)], the kinetic evolution of the coloured MH^+ form is described by eqn. (7).

$$\frac{d[M]}{dt} = k_1[SO] - k_2[M]\cdot[H^+] - k_{-1}[M] = 0 \qquad (6)$$

$$\frac{d[MH^+]}{dt} = \frac{k_1k_2[H^+]\cdot[SO]}{k_{-1}+k_2[H^+]} - k_3[MH^+] - k_4[MH^+][H^+] \qquad (7)$$

To integrate this equation, some reasonable approximations can be introduced. Since the protonation reaction (2) is much faster than the ring-closure process ($k_{-1} \sim 10^{-1}$ s^{-1} at room temperature), k_{-1} can be neglected with respect to $k_2[H^+]$. Depending on whether the acid is in stoichiometric amount or in excess, the bleaching process is governed by either eqn. (3) (with the rate $k_3[MH^+]$) or eqn. (4) ($k_4[MH^+][H^+]$). In both cases the colouration and decolouration steps occur over different time scales, as shown by the experimental kinetic evolution of the absorbance of the colour band (Fig. 8). This allows the two processes to be considered separately.

Based on these assumptions, the colour forming kinetics are described by eqn. (8), where [SO] is expressed in terms of the initial SO concentration, C_0, and the MH^+ concentration.

$$\frac{d[MH^+]}{dt} = k_1[SO] = k_1(C_0 - [MH^+]) \qquad (8)$$

Eqn. (8) can be easily integrated in the $[0,t']$ interval, giving eqn. (9):

$$[MH^+]_{t'} = C_0 + \left([MH^+]_0 - C_0\right)e^{-k_1t'} \qquad (9)$$

This equation can be expressed in terms of absorbances (ε_{MH^+} is the MH^+ molar absorption coefficient and l is the optical path), as in eqn. (10):

$$A^{t'}_{MH^+} = \varepsilon_{MH^+}lC_0 + \left(A^0_{MH^+} - \varepsilon_{MH^+}lC_0\right)e^{-k_1t'} \qquad (10)$$

For the bleaching kinetics the behaviour of diluted and concentrated acid solutions is different.

In the dilute acid solution, only eqn. (3) is considered, which is kinetically described by the monoexponential functions of eqns. (11) and (12) (the latter in terms of absorbances):

$$[MH^+]_{t''} = [MH^+]_{t'}e^{-k_3(t''-t')} \qquad (11)$$

$$A^{t''}_{MH^+} = A^{t'}_{MH^+}e^{-k_3(t''-t')} \qquad (12)$$

When the acid is in great excess compared to SO, a second protonation [eqn. (4)] occurs subsequently to the initial protonation in eqn. (2). Since no new colour band was observed, it can be argued that MH_2^{2+} rapidly closes to form SOH_2^{2+} [eqn. (5)], without accumulating. The temporal variation of MH^+ is given by eqn. (13), where $C_{HClO_4} \approx [H^+]$.

$$-\frac{d[MH^+]}{dt} = k_4[MH^+]\cdot[H^+] = k_4[MH^+]\cdot C_{HClO_4} \qquad (13)$$

By integrating in the interval $[t',t'']$, eqn. (14) (in terms of absorbances) is obtained:

$$A^{t''}_{MH^+} = A^{t'}_{MH^+}e^{-k_4C_{HClO_4}(t''-t')} \qquad (14)$$

By convoluting the functions describing the colouration [eqn. (10)] and decolouration [eqns. (12) and (14)] steps, eqns. (15) and (16) are obtained, which describe the overall kinetics in diluted acid solution and in concentrated acid solution, respectively:

$$A^t_{MH^+} = \left[\varepsilon_{MH^+}lC_0 + \left(A^0_{MH^+} - \varepsilon_{MH^+}lC_0\right)e^{-k_1t}\right]e^{-k_3t} \qquad (15)$$

$$A^t_{MH^+} = \left[\varepsilon_{MH^+}lC_0 + \left(A^0_{MH^+} - \varepsilon_{MH^+}lC_0\right)e^{-k_1t}\right]e^{-k_4C_{HClO_4}t} \qquad (16)$$

The recorded data in Fig. 8(a) and 8(b) are thoroughly described by the functions given in eqns. (15) and (16), respectively. By fitting several sets of experimental data, the values for the rate constant of the thermal opening reaction, k_1, obtained for the two different acid concentrations, were found to be in excellent agreement [$k_1 = (1.020 \pm 0.005) \times 10^{-3}$ s^{-1} in diluted acid solution and $k_1 = (1.010 \pm 0.003) \times 10^{-3}$ s^{-1} in concentrated acid solution]. Since the colouration step proceeds at the same rate when $HClO_4$ is added either in strong excess or in stoichiometric amount, the assumption of neglecting the ring-closure reaction of M to SO (represented by k_{-1}) with respect to the first protonation process ($k_2[H^+]$), is indirectly confirmed. If this assumption was not correct, the rate of colouration would depend on acid concentration. The rate constant for thermal closure of MH^+, $k_3 = (4.8 \pm 0.1) \times 10^{-6}$ s^{-1}, was determined from the low acid concentration kinetics [eqn. (15), Fig. 8(a)], while the rate constant for MH^+ protonation, $k_4 = (2.777 \pm 0.002) \times 10^{-2}$ s^{-1} dm^3 mol^{-1}, was obtained from the strongly acidified solution [eqn. (16), Fig. 8(b)].

The k_1 value is about two orders of magnitude greater than in ethanol[11] and about three orders of magnitude greater than in toluene.[11] These differences can be attributed to the different polarities of the solvents.[11] In this work, k_1 was determined in a polar solvent, CH_3CN, containing a strong electrolyte, $HClO_4$, which creates a highly polar environment that could accelerate the SO → M conversion.

The very slow process of MH^+ closure to give SOH^+ (rate constant k_3) in CH_3CN recalls the even slower closure reaction observed in the solid phase. It is noteworthy that the long time required to convert MH^+ into SOH^+ (several days) favours secondary oxidation reactions. If NaOH is added before side processes occur, the colour band rapidly disappears and a

SO solution is obtained. In other words, the chemical system shows acid-base reversibility in the case of "soft" acidification, when SOH_2^{2+} is not produced.

The fitting procedure, performed at various wavelengths of the colour band, also allowed the molar absorption coefficients of MH^+ to be determined (Table 2).

The final product in very acid solution (SOH_2^{2+}) did not absorb in the visible region but emitted visible light. Upon UV irradiation its spectrum changed due to a photochemical reaction yielding unidentified side products. The fluorescence and fluorescence excitation spectra of SOH_2^{2+} are shown in Fig. 9, together with the absorption spectrum. The patterns of the fluorescence excitation and absorption spectra were independent of the monitoring and exciting wavelengths, respectively, indicating that the emission is due to a unique fluorophore. By comparing the relative intensities of the vibronic peaks of the absorption and excitation spectra, it can be deduced that the fluorescence quantum yield (Φ_F) depends on λ_{exc}. The Φ_F values, at different excitation wavelengths, corresponding to the peaks of the fine structure, are reported in Table 2. As the excitation energy increased, the Φ_F value decreased about threefold. As proposed for other organic molecules, this behaviour is due to competition between radiative relaxation and photochemistry at each vibronically excited level.[31,32] A tentative structure for SOH_2^{2+} (Scheme 3) can be proposed by considering that protonation of the MH^+ imine nitrogen makes the C(2′) atom more electrophilic; it is easily attacked by oxygen, thus determining cyclization followed by "pinacolic" hydrogen transposition from C(2′) to C(2). A similar structure was previously proposed in the literature[33] for a fluorescent photoproduct obtained by UV irradiation of SO in an air-equilibrated acetonitrile solution. The absence of extended electronic conjugation enables SOH_2^{2+} to absorb visible light, while the presence of two rigid annular structures justifies the vibrational resolution of the absorption spectrum.

Table 2 Spectral properties of MH^+ and SOH_2^{2+}. Fluorescence quantum yields (Φ_F) as a function of λ_{exc} for SOH_2^{2+}. The uncertainties on ε are the average standard deviations of different measurements

MH^+		SOH_2^{2+}		
λ/nm	ε/dm^3 mol^{-1} cm^{-1}	λ_{exc}/nm	ε/dm^3 mol^{-1} cm^{-1}	Φ_F
470	9400 ± 500	330	2700 ± 30	0.098
511	13 400 ± 400	316	3480 ± 40	0.058
550	8200 ± 400	286	8640 ± 70	0.040
		274	9500 ± 80	0.040
		264	7740 ± 60	0.037

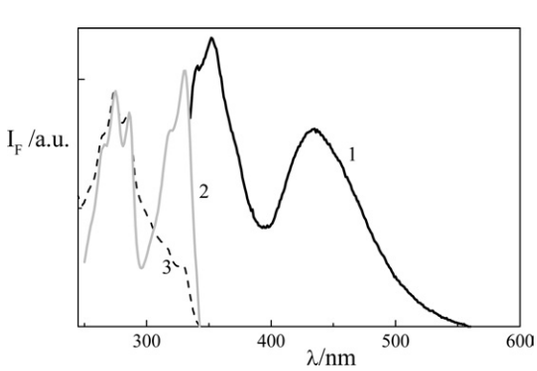

Fig. 9 Fluorescence (1; $\lambda_{exc} = 286$ nm), fluorescence excitation (2; $\lambda_{em} = 441$ nm) and absorption (3) spectra of SOH_2^{2+}.

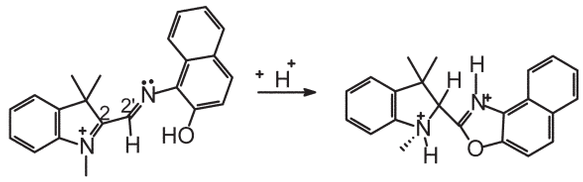

Scheme 3

Conclusions

Microcrystalline SO powder was shown to exhibit unusual chromogenic properties that could have promising applications. It is sensitive to different external stimulations: colouration can be produced by UV irradiation, by increasing pressure and by lowering the environmental pH. Thus, it can be defined as a "multi-way" optically switchable material.

SO crystalline powder is photochromic. Coloured M was produced not only by intense laser excitation[16,17] but also by steady UV irradiation.

Furthermore, it is piezochromic. Pressure forces the molecular system into the flat M conformation. Piezo-merocyanines were produced by applying a mechanical force. When the exciting light or mechanical perturbation was discontinued, spontaneous thermal bleaching was observed, at room temperature, in the dark. This is the slowest closure process that has ever been reported in the literature for the fading of SO in several different micro-environments. The kinetics are biexponential and this is explained by assuming the formation of M spots in the crystalline phase: a few, random SO molecules, converted to planar merocyanines by the external perturbation, act as "nucleation centres" for producing other planar Ms, which lead to spot formation. When the perturbation is interrupted, the M → SO conversion can occur. Since the internal Ms are less constrained than those at the border, they undergo the closure reaction more rapidly.

SO powder was also found to be acidichromic. SO extracted protons from an acidic solid matrix, ZrP, simply by being in physical contact with it. Proton transfer was enhanced by manual crushing of the powdery SO–ZrP mixture. The maximum colour intensity induced by acid perturbation is attained after several hours. As colour saturation is achieved, slower decolouration followed. This kind of colouration dynamics was observed even in SO acidified solutions; the time scale of the spectral evolution is somewhat shorter than that in the solid phase. In solution, the colouration rate is independent of the $HClO_4$ concentration since the rate-determining step is the SO → M ring-opening reaction. The decolouration step depends on the acid concentration. When the amount of $HClO_4$ is nearly equimolar with SO, M monoprotonation occurrs, followed by a rather slow closure reaction, with colour disappearance. When $HClO_4$ is in excess, M is doubly protonated, followed by fast, irreversible ring closure.

Acknowledgements

This research was funded by the Ministero per l'Università e la Ricerca Scientifica e Tecnologica (Rome) and the University of Perugia in the framework of the Programmi di Ricerca di Interesse Nazionale (project: "Photoprocesses of interest for applications") and of the FIRB project "Spectroscopic and kinetic study of organic photochromic compounds in solution, microheterogeneous media and polymeric films". It was also partially funded by the Italian Consiglio Nazionale delle Ricerche in the framework of the Progetto Finalizzato "Materiali Speciali per Tecnologie Avanzate II".

References

1 C. B. Greenberg, *Thin Solid Films*, 1994, **251**, 81.
2 J. Scott, M. Asami and K. Tanaka, *New J. Chem.*, 2002, **12**, 1822.
3 Y. P. Kovtun, Y. O. Prostota and A. I. Tolmachev, *Dyes Pigm.*, 2003, **58**, 83.
4 G. Beni and J. L. Shay, *Adv. Image Pickup Display*, 1982, **5**, 83.
5 W. R. Roach, *Appl. Phys. Lett.*, 1971, **19**, 453.
6 A. W. Smith, *Appl. Phys. Lett.*, 1973, **23**, 437.
7 I. Balberg and S. Trokman, *J. Appl. Phys.*, 1975, **46**, 2111.
8 N. Y. C. Chu, *Can. J. Chem.*, 1983, **61**, 300.
9 A. Kellmann, F. Tfibel, R. Dubest, P. Levoir, J. Aubard, E. Pottier and R. Guglielmetti, *J. Photochem. Photobiol., A*, 1989, **49**, 63.
10 F. Wilkinson, J. Hobley and M. Naftaly, *J. Chem. Soc., Faraday Trans.*, 1992, **88**, 1511.
11 G. Favaro, F. Masetti, U. Mazzucato, G. Ottavi, P. Allegrini and V. Malatesta, *J. Chem. Soc., Faraday Trans.*, 1994, **90**, 333.
12 A. Samat and V. Lokshin, in *Organic Photochromic and Thermochromic Compounds*, eds. J. C. Crano and R. J. Guglielmetti, Kluwer Academic, Plenum, New York, 1999, vol. 2, ch. 10.
13 X. D. Sun, M. G. Fan, X. J. Meng and E. T. Knobbe, *J. Photochem. Photobiol., A*, 1997, **102**, 213.
14 P. Rys, R. Weber and Q. Wu, *Can. J. Chem.*, 1993, **71**, 1828.
15 S. Bernard and Y. Yu, *Adv. Mater.*, 2000, **12**, 48.
16 T. Asahi, M. Suzuki and H. Masuhara, *J. Phys. Chem. A*, 2002, **106**, 2335.
17 M. Suzuki, T. Asahi and H. Masuhara, *Phys. Chem. Chem. Phys.*, 2002, **4**, 185.
18 L. S. Kol'tsova, N. L. Zaichenko, A. I. Shiyonok and V. S. Marevtsev, *Russ. Chem. Bull.*, 2001, **50**, 1214.
19 M. Fan, X. Sun, Y. Liang, Y. Zhao, Y. Ming and E. T. Knobbe, *Mol. Cryst. Liq. Cryst.*, 1997, **298**, 29.
20 Y. Liang, Y. Ming and M. Fan, *Sci. China, Ser. B*, 1997, **40**, 535.
21 G. Alberti and E. Torracca, *Inorg. Nucl. Chem.*, 1968, **30**, 317.
22 W. H. Melhuish, *J. Phys. Chem.*, 1961, **65**, 229.
23 G. Kortuem, *Reflectance Spectroscopy*, Springer-Verlag, Berlin, Heidelberg, New York, 1969.
24 P. L. Gentili, U. Costantino, M. Nocchetti, C. Miliani and G. Favaro, *J. Mater. Chem.*, 2002, **12**, 2872.
25 G. Favaro, F. Ortica and V. Malatesta, *J. Chem. Soc., Faraday Trans.*, 1995, **91**, 4099.
26 G. Favaro and F. Ortica, *J. Phys. Chem. B*, 2000, **104**, 12 179.
27 S. Nakamura, K. Uchida, A. Murakami and M. Irie, *J. Org. Chem.*, 1993, **58**, 5543.
28 V. Malatesta, G. Ranghino, U. Romano and P. Allegrini, *Int. J. Quant. Chem.*, 1992, **42**, 879.
29 J. M. Troup and A. Clearfield, *Inorg. Chem.*, 1977, **16**, 3311.
30 G. Alberti, M. Casciola, U. Costantino, G. Levi and G. Ricciardi, *Inorg. Nucl. Chem.*, 1978, **40**, 533.
31 R. S. Becker, A. P. Pelliccioli, A. Romani and G. Favaro, *J. Am. Chem. Soc.*, 1999, **121**, 2104.
32 G. Favaro, A. Romani and R. S. Becker, *Photochem. Photobiol.*, 2000, **72**, 632.
33 V. Malatesta, *Mol. Cryst. Liq. Cryst.*, 1997, **298**, 69.